A novel low-profile shape memory alloy torsional actuator

A novel low-profile shape memory alloy torsional actuator

Jamie K Paik[1]**, Elliot Hawkes**[1,2] **and Robert J Wood**[1]

[1] School of Engineering and Applied Sciences, Harvard University, Cambridge, MA 02138, USA
[2] Stanford University, Palo Alto, CA 94305, USA

E-mail: jpaik@seas.harvard.edu

Abstract

This paper presents low-profile torsional actuators applicable for mesoscale and microscale robots. The primary actuator material is thermally activated Ni–Ti shape memory alloy (SMA), which exhibits remarkably high torque density. Despite the advantages of SMAs for actuator applications—high strain, silent operation, and mechanical simplicity—the response time and energy efficiency limit overall performance. As an alternative to SMA wires, thin SMA sheets are used to fabricate effective yet compact torsional actuators. Also, instead of using conventional Joule heating, an external Ni–Cr heating element is utilized to focus heat on the regions of highest required strain. Various design parameters and fabrication variants are described and experimentally explored in actuator prototypes. Controlled current profiles and discrete heating produces a 20% faster response time with 40% less power consumption as compared to Joule heating in a low-profile (sub-millimeter) torsional actuator capable of 180° motion.

(Some figures in this article are in colour only in the electronic version)

1. Introduction

Shape memory alloys (SMA) are attractive engineering materials due to the ability to memorize shapes through a thermally induced solid state phase transition. Among several industrially developed SMAs (Cu–Zn–Al, Cu–Al–Ni, Ni–Ti), the most common SMA is Ni–Ti (Nitinol) alloy used for its ductility and fatigue and corrosion resistance [1, 2]. SMA has two phases: low-temperature martensite and high-temperature austenite. Heating past the alloy's transition temperature results in a change in the crystal structure, in which the martensite composition of the alloy turns into austenite crystals. This shift is called 'twinning' and a shape change is associated with this twinning. After cooling, 'twinned (or self-sustaining) martensite' can be deformed by load and this phase is called 'deformed (or de-twinned) martensite'. Upon heating again, this deformed martensite can return to the initial austenite phase shape. A useful feature of SMA is that the austenite shape can be reset through an annealing process. In this process, the SMA is secured in the desired shape, then annealed at high temperature (well above the transition temperature) where a new crystal structure is set to form a new austenite phase shape. This annealing process resets the shape that is memorized.

SMA materials are readily available in multiple initial forms such as wires, tubes, and sheets. Its use in actuators has gained popularity, especially in low volume constraint applications, such as medical catheters, stents (thin wires, mesh form) [3–5], laparoscope surgical tools (patterned tubing, wires) [6], and micro-robot actuators (coiled wires) [7, 8]. Wires are a more common form of actuators, but they are essentially one-dimensional structures while sheets enable a two-dimensional design space [9–11]. As with all fabrication processes, both machining and assembling steps are critical in achieving mechanically and functionally consistent results. However, due to the scale of the desired microstructures, alignment and component stability present more critical issues. A possible solution is to machine all parts at once (eliminating need for the alignment) and minimizing number of assembly components. Flat sheet SMA is attractive for high resolution laser machining without having to reposition the material or worry about thermal effects of machining. An effective 2D design can achieve 3D shape and motions by folding out of the plane. In this paper, we present an actuator fabrication process

that can be embedded in such 2D sheets. We also characterize novel folding actuator prototypes that are machined from flat SMA sheet and capable of producing 0–180° motion with high torque density and a low (close to 500 μm in total thickness) profile.

2. Related work in SMA actuators

While many researchers have utilized SMA materials as actuators, there is no standard model which prescribes temperature, load, and material geometry for a desired performance; the convention therefore is to derive an actuator model's thermo-mechanical properties experimentally, either partially or fully [12–23]. SMA actuators have found a wide spectrum of applications in small-scale devices. For instance, in biomimetic locomotion, SMA exhibits muscle-like strain and strain-rate properties. Menciass and Kim [24, 25] demonstrated an earthworm-like robot, and Koh [26] a multi-DOF inchworm with the use of SMA muscles (SMA wires). Yang [13] created a jellyfish robot, using SMA to alter the shape of an orifice, which then allowed the device to pump water while swimming. A micro-robot fish [27] uses segmented motions of multiple SMA wires to propel the body under water. As instruments, a miniature gripper [28], automotive tumble flaps [29], and a control valve for automobile engines [8] also use SMA wires in for actuation. A torsional spring type actuator is seen in modular robots as well [7]. Although SMA wires are a popular form of actuation, their design space is limited to 1D. In order to overcome this limitation, wires are used in multiple orientations and numbers [30–33] or even with different material properties (using both shape memory and superelastic properties of Nitinol [34]) to produce desired motion. However, 2D and 3D material choices (i.e. SMA tubes, sheets, ribbons) can overcome design space limitations and often alleviate spatial and geometrical challenges. Nakamura uses SMA sheets to make flat springs, where a section of SMA is patterned such that the remaining material works as a two-dimensional actuator [11]. A bending mechanism using a simple pin joint utilized flat SMA and placed actuators on both sides of the pivot to create rotational motion [35]. There also has been efforts in thin-film SMA actuators (thickness of 10–20 μm) where the alloy composition and beam shapes determine the actuator properties [36–39, 2]. There has been only minimal use of 3D materials for creating actuators. In one example, an SMA tube, Tung made a bending catheter by patterning sections of the tube, instead of a flat sheet [4]. In 2D and 3D design spaces, the actuators have more independent design choices than SMA wires while having a variety of form factors.

An actuator with high torque density and low profile is a paradoxical design problem as typical methods of torque amplification involve elongating a moment arm. One of the most extreme physical applications for actuators would be a self-folding origami sheet [40]. In such applications, the actuators must be small enough to be embedded within the substrate material while sufficiently powerful to achieve folding. Existing SMA sheet actuators may have high torque density [11, 30, 35, 4] but often lack the range of motion that
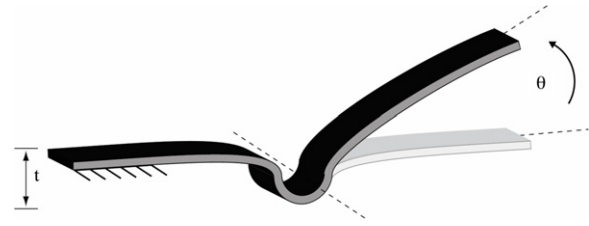

Figure 1. Folding axis and motion definition of actuators. The profile thickness of the actuator, t, is approximately 500 μm.

would execute the motion of folding (at least 180°). The range of motion can increase with coiling, using gears, or changing winding types [41], but then the spatial form factor becomes larger than that of a thin sheet. Our design achieves thin form factor SMA actuators (500 μm in total thickness) to produce large rotations with high torque density.

3. Actuator design and fabrication

In efforts to increase the strain in SMA, which is typically around 8% for NiTi [42], many actuator designs employ SMA in wire or coil forms. As a thin wire, the aggregate force and displacement properties can be adjusted by spooling the wire around a rotating core and annealing in this coil shape [43]. For wires, coiling can multiply the given strain proportionally to the number of turns in the coil. In a wire or in coil form, the actuators undergo transformation strains, including the transformation volume strain as well as shear strain. SMAs in thin sheet forms have an attractive shape for a thin and compact actuator; however, such shape only undergoes a volumetric transformation without shear strain, making the overall strain smaller than a coiled SMA. Although it is challenging to use sheets as actuators, a flat shape is attractive for space-limited applications and monolithic fabrication processes. Here, we present designs which optimize performance of a thin sheet actuator through folding and annealing.

3.1. Design parameters

The SMA torsional actuator presented in this paper uses a unique design and annealing method to maximize torque and the range of motion (see figure 1 for definitions). A complete torsional actuator can be cut out from a single sheet with a laser and requires minimal assembly. Due to the specific annealing method, the actuators take two designs that resemble the letters Y and Z (figure 2). These shapes accommodate the interlacing annealing method for maximizing the applied strain (i.e. fixturing during annealing requires greater than 360° folds, thereby requiring geometries which would not self-intersect when folded). Furthermore, for Joule heating, it is most convenient to have both electrodes on the same side of the joint in order to maximize the length of, and hence resistance of the circuit path and for convenient connection to the rest of the circuit, hence the Y shape (see figure 7 for simulated thus for 'Y' and 'Z' type). The total resistance of the structure is critical when Joule heating the actuator; the higher the resistance, the faster the rate of temperature increase
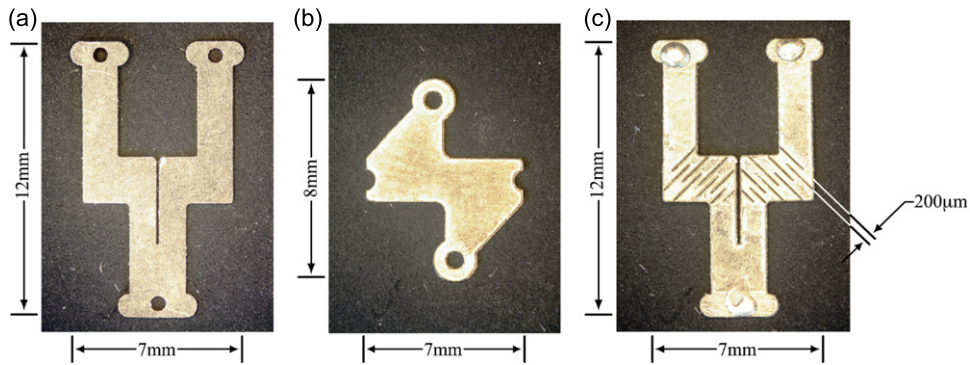
Figure 2. SMA torsional actuator types. (a) Y-type, (b) Z-type and (c) Y-type, with ribbed pattern for a maximal resistance path.
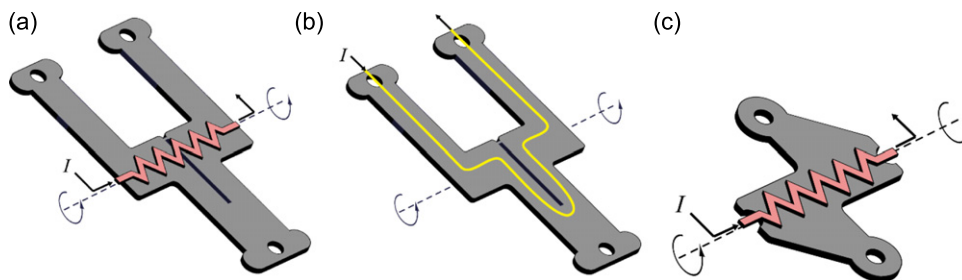

Figure 3. Electrical circuit representation of the models. (a) Y-type: Ni–Cr heating, (b) Y-type: Joule heating and (c) Z-type: Ni–Cr heating.

to activate the actuator. Figure 2(b) shows an example of a Y-type actuator with a ribbed midsection in an effort to maximize this resistance path. Although the ribbed design isolates the heating in the midsection where the folding occurs, the feature also weakens the mechanism. A Z-type actuator forgoes a long resistance path since external heating coils now trigger the phase change instead of Joule heating. During the annealing process, it is important to keep the radius of curvature of the actuator's folding edge constant, not only for its post-annealed mechanical performance but also for fitting the heating coil in the area of curvature. The annealing process ensures a constant center of rotation and a constant radius of curvature by proper fixturing as described in section 3.2. There are actually three areas of actuation that allow for a full 180° motion. The first is the central fold (a 500 μm radius of curvature, rather than a flat fold), and the other two are the opposite curvatures on either side of the central fold. Figure 1 illustrates the actuator's central folding axis and the direction of the motion.

Our designs use a 100 μm thick Ni–Ti sheet with a 55–65 °C martensite–austenite transformation temperature (type M alloy [42]). This material choice was based upon availability of sheet thicknesses and maximum machinable depth that we can attain from laser machining (details in section 3.2). The design parameters of the 12 mm tall, Y-shaped annealed actuators are determined by the maximum length of the electric current path through the electrodes while minimizing the overall actuator size subject to practical constraints such as anchoring and integration. The phase transition in SMA actuators is thermally activated, often by Joule heating. The absolute resistance of the actuator can be chosen based upon a material's innate electrical resistivity or geometry. Higher resistivity produces greater power dissipation at lower currents which could be important for minimizing I^2R losses in neighboring circuits. Furthermore, if resistance can be patterned in specific areas, such as the actuation area, heating can be isolated from the rest of the body (see figure 2(c)). The prototypes (figure 2) have pre-drilled holes for bolts (0.5 mm pitch diameter), which eliminates complexity in mounting to the substrate. Riveting and/or bolting instead of soldering minimize the localization of solder resistance and cold solder joints, while fixing the actuator to the folding edges of a flat substrate (e.g. robotic origami prototype). Using bolts and nuts as shown in figures 4(b) and (c) to fix the actuators provides better electrical connections and flush surfaces for folding.

One of the key drawbacks of SMA actuators is their slow response time, which depends on the thermodynamics of the heating method and the consequent martensite-to-austenite transformation rate (which varies according to material composition, thickness and annealing condition). The most widely used SMA actuation method is using the actuator body as the resistance in the electrical circuit (Joule heating). However, as table 1 shows, when the actuator uses the internal Joule heating of the Ni–Ti material, a substantial current is typically required. This high current can cause problems for associated electrical traces due to I^2R losses. Instead of utilizing actuator legs as electrodes, a Ni–Cr heater coil only heats the hinge area for effective and rapid heat transfer for actuation. Furthermore, as the actuator is no longer part of the circuit, only two ends need to be fixed to the substrate at opposite sides of the actuated joint. The elimination of electrodes simplifies the shape and enables
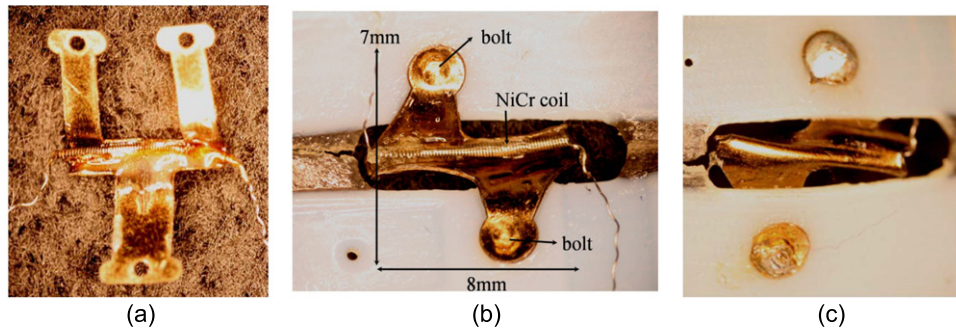
Figure 4. SMA torsional actuators with Ni–Cr heating coil. (a) Y-type and (b), (c) Z-type: bolted down front and back view.
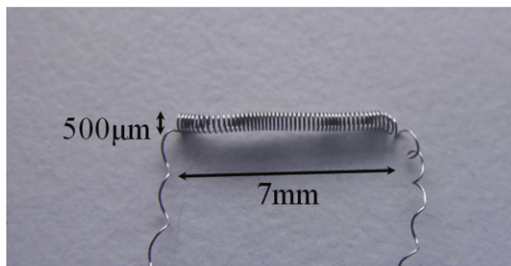

Figure 5. Ni–Cr coil (gauge 40 wire).

Table 1. Electrical resistivity, ρ, for the materials considered.

Material	Resistivity (10^{-9} Ω m)
Cu	17.1
Ni–Ti	80–100
Ni–Cr	1500

Table 2. Z-type design, maximum strain for annealing geometry and target range of motion.

Rod diameter (mm)	Strain (%)	Range of motion (deg)
0.90	11	180
1.30	7	130
1.90	5	100

further miniaturization. Figure 3 illustrates the different thermal activation methods and corresponding heating paths on the actuator body.

3.2. Fabrication process

One goal of creating the torsional SMA actuator is to simplify the fabrication process of the device in relation to SMA spring actuators and other rotational motors. Ideally, all actuator designs should be rapidly and repeatedly batch processed and easily embedded into the structure of the actuated body. Keeping this goal in mind, we fabricate the actuators in four steps. The first step of the process involves laser machining the SMA sheet. The sheet is mounted on a glass slide with an adhesive film (X-8 by Gel-Pak Co.) and cut with a diode-pumped solid state Q-switched, pulsed Nd:YVO$_4$ (neodymium doped yttrium vanadate crystal, 355 nm) laser micromachining system (figure 6(a)). The laser has a spot size of 10 μm and runs at 20 kHz pulserates and 0.15 m s^{-1} cutspeed. For our application, photoetching processes [39, 38, 2] are not desirable due to large material thickness (150 μm). However, we have found no significant deterioration in SMA performance due to the laser heat affected zone [44, 45, 5, 36, 2]. A series of actuators are cut side-by-side, connected by small tabs. This connection

allows the following steps to work as a batch, rather than on individual actuators, consequently minimizing fabrication time and variability.

The second step involves bending the cut SMA and placing it into a jig. The SMA is scored and bent using a small sheet metal bender. Once there is a crease, the actuators are further bent around a cylindrical rod until a nearly 360° loop is achieved (figure 6(b)). SMA never returns fully to its annealed position [12] due to its innate elasticity that does not disappear completely even after annealing, so in order to attain a certain range of motion, the actuator must be annealed beyond this range. Table 2 shows the effect of the annealing rod size on the degree of range of motion of the actuator.

The bent set of actuators is placed in the jig, which has three sections (figure 6). The loop is clamped between the bottom two sections, and the two arms are secured by the top section. The jig is made of three pieces of steel bolted together with a slot for a central rod to sit. While tightening the jig, the steel rod is slipped into the loop to maintain a minimum radius of curvature (this is also where the heating coil sits). This is crucial in preventing the SMA from fraturing along too sharp of a crease. Annealing is the third step: the set of actuators and the jig are placed in a furnace and heated at 400 °C for 30 min [46, 47]. The annealing process is the same for both Y- and Z-shaped actuators, as the jig only holds the cutouts about the folding axis figure 6(b). During this annealing process, we are creating a new 'memory' for the actuators, and also eliminating the heat affected zone created by the previous laser machining process. The final step is unfolding the annealed set of actuators to prepare them for mounting. Once removed from the jig, the arms of the actuators are brought past each other to unfold the 360° loop (see figure 6(c)). Due to the properties of SMA, after this de-twinning, the actuators remain in the open position with no external force until heated beyond the transition temperature. This open position enables easy mounting to a body (figure 6(d)). For actuators with external
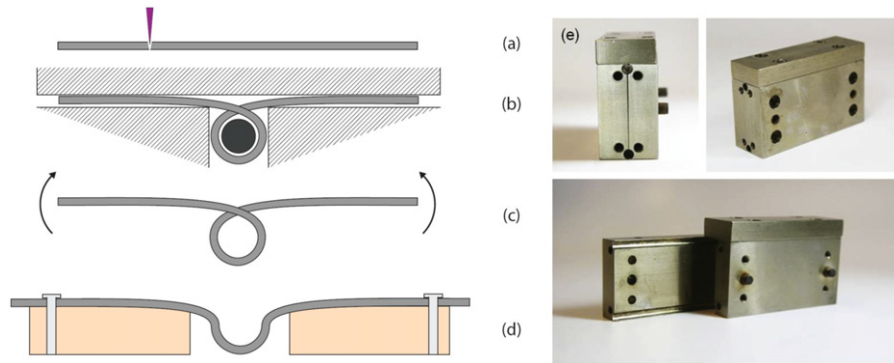
Figure 6. SMA fabrication process for maximizing annealing angles and the annealing jig. (a) Laser cutting the pattern from SMA sheet, (b) annealing the actuators in the jig with a wrapping rod inserted, (c) unwrapping the annealed actuator flaps, (d) mounting the actuator, and (e) assembled and disassembled annealing jigs.
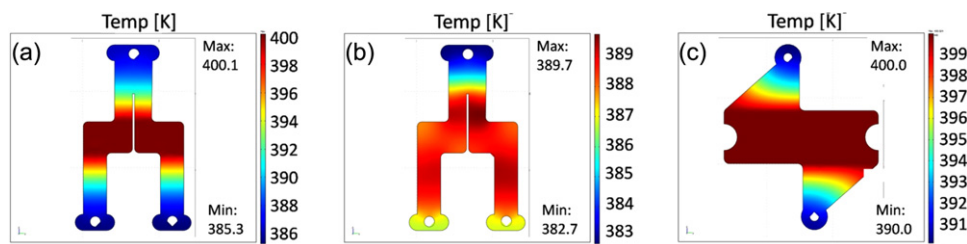

Figure 7. COMSOL simulation of heat distribution in the actuators. (a) Y-type: Ni–Cr heating, (b) Y-type: Joule heating and (c) Z-type: Ni–Cr heating.

heating elements, heating coils are glued with thermal epoxy (50-3150 FR, Epoxies Co.) to the SMA actuator's folding edge. Table 3 shows different Ni–Cr (A-type: 80% Ni, 20% Cr) wires that were considered and tested for their application as miniature heaters for the thermal activation. All the heating coils are formed by winding around a 0.5 mm rod in the center (figure 5) and stretched out to have the same pitch as the diameter of the wire. The current required to reach 100 °C are shown the last column of table 3. Table 4 shows the dimensions and total weight of the actuators with the heater. The length of the coil matches the dimensions of the actuators Y and Z. Figure 4 displays Y and Z-type actuators with heating coils attached to the folding edges. Since the thermally conductive epoxies take on average 24 h to cure, the coil is placed and clamped at the proper groove until it is fixed. Bolts and nuts are used to affix the actuators onto the robotic origami's folding edges. The derived dimensions for Y and Z-type actuators are chosen for effective heating (both Joule heating and external coil heating), torque, and range of motion while considering the ease of annealing, fixation, and manipulation of the actuators during fabrication. In the interest of miniaturization [48, 49], we are using the smallest actuators for generating maximal torque for a self-folding structure, given the limitations of the fabrication steps described above.

Figure 7 compares the temperature gradients of the actuators, depending on the thermal actuation method. Due to the location of the electrodes, the Y-type actuator without the heater has uniform heating along the full path of the circuit. The Y-type and Z-type with heaters display concentrated heating at the actuating edge, where the deformation occurs. In

Table 3. Properties of Ni–Cr A-type wire coils.

AWG (gauge) (diameter (mm))	$\Omega\ \mu m^{-1}$	Current at 100 °C at 20 V (A m^{-1})
40(0.078)	220	1.24
36(0.127)	85	3.17
30(0.254)	21	15.8

Table 4. Prototype actuator dimensions (100 μm thickness).

Shape	Activation method	Total weight (10^{-3} kg)	Dimensions (mm)
Z	Ni–Cr coil heating	0.035	8 × 7
Y	Ni–Cr coil heating	0.033	12 × 7
Y	Joule heating	0.025	12 × 7

these steady state COMSOL simulations, Joule heating in the Y-type actuator shows a broader heat distribution throughout the body compared to those of Z-type and Y-type actuators with a 400 K external heater. Selective heating is desirable for rapid heating of the SMA material, shorter cooling time, and greater efficiency.

4. Actuator experiments and discussions

The phase change of SMA material is responsible for its attractive thermo-mechanical memory properties; however, it also introduces diverse interpretation for material modeling which are dependent on load, shape, time, composition, and temperature. We are interested in the typical actuator metrics:
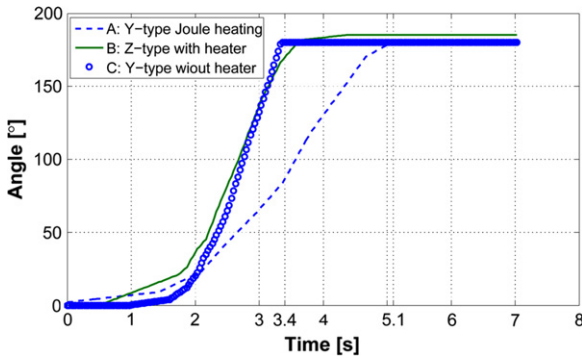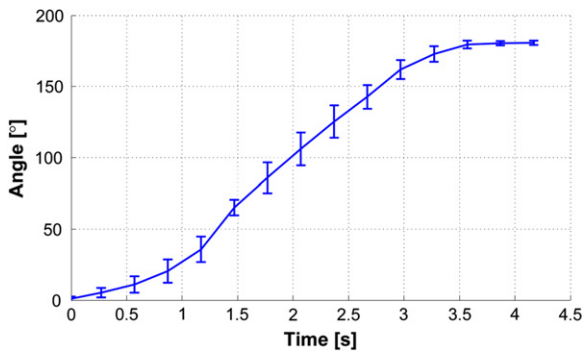
Figure 8. Sample actuator step responses.

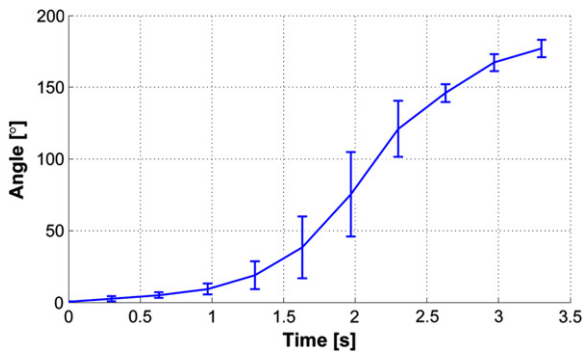**Figure 9.** Single Z-type actuator repeatability (13.9 V at 0.17 A).

Figure 10. Six samples of Z-type actuator (supplied 13.9 V at 0.17 A).

Figure 11. Temperature and angular velocity of the Y actuator. (a) Angle versus temperature and (b) temperature, angle versus time.

Figure 12. Experimental setup for measuring blocked torque. A actuator mounted on a gripper is deflected while a known current is applied and the load on a point recorded.

torque, displacement, efficiency time constant, and power. For this, we characterized the dynamic response of different modes of actuation and the quasi-static response using a blocked torque measurement.

4.1. Dynamic testing

In order to understand the actuator's dynamic response and to assess the consistency of fabrication, we measured the actuator's step response, repeatability, and angular deflection rate to temperature changes. For dynamic testing, there is no external load on the actuator other than its own weight which is neglected because of the scale of the actuators.

One of the most common drawbacks for SMA actuators is their slow response time. Using an external Ni–Cr heating coil, our actuator displayed a 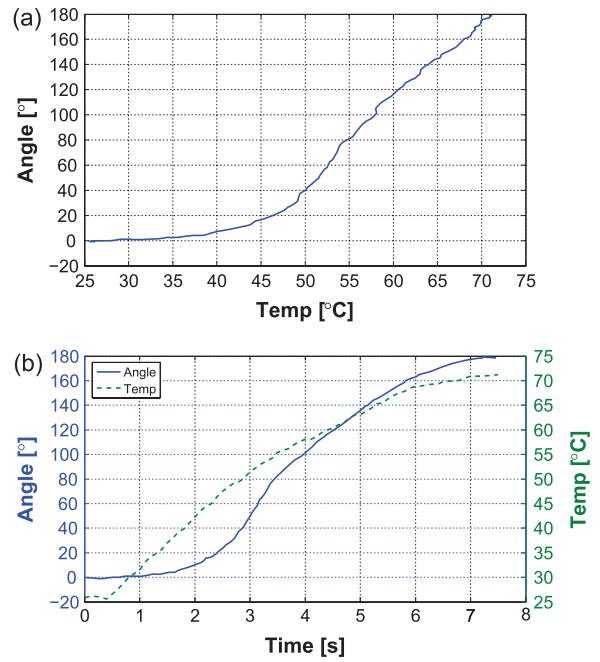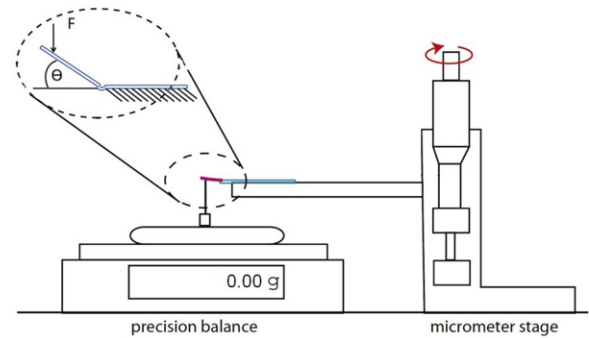significantly improved response, with approximately 20% decrease in response time compared to Joule heating (figure 8). Here, different levels of step current were fed to the actuators. We performed the testing under current control, in which the actuators with heating coils had a current control 0.19 A at 13 V, and Y-type without a heater had the current controlled at 2.6 A with 13 V. In order to maximize the speed of the step response, we increased the current level until the actuator would not perform any faster due to the thermal conduction rate. Increasing the power did not show significant speed change. It is generally acknowledged that the volume fractions of the martensite and austenite composition determine the temporal properties of the actuator motion [12, 16]. For a Joule-heated actuator, this composition change depends proportionally on the thickness, shape, and the circuit length. However, the heating coils provide localization of the heating at the folding joint and this accelerates the crystal transition rate at the specific area.
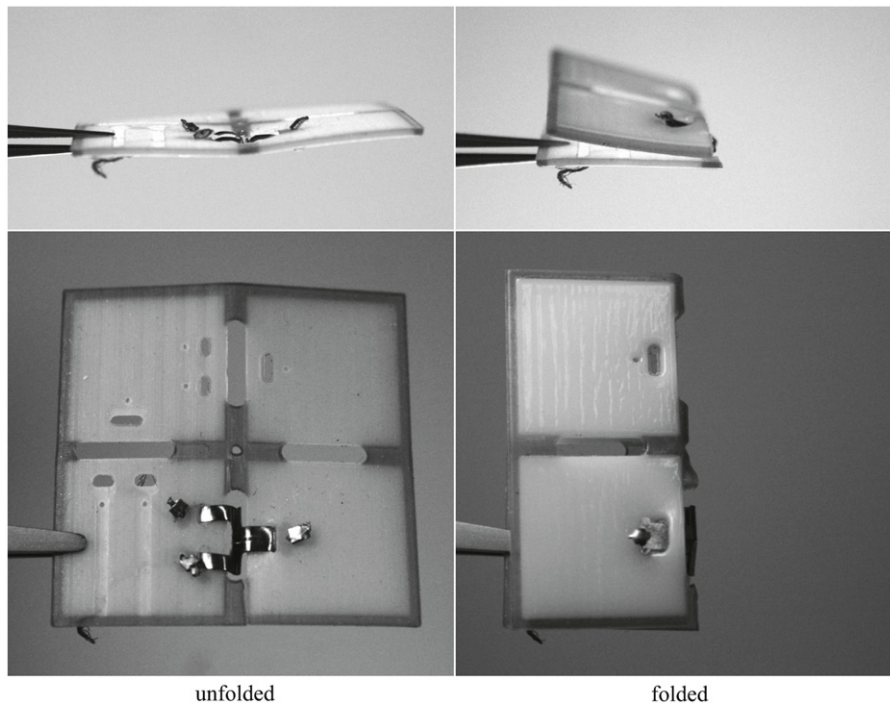
6

unfolded   folded

Figure 13. Two positions of an actuated robotic origami [40].

According to the Ni–Ti material property documentation, up to 5% working strain is allowed for less than 100 fatigue repetitions, and at any given time the maximum strain should be 8%. We observed a sample of the Z-type actuator's angular deflection rate to determine how viable the fabrication method is for producing consistent mechanical outputs, while keeping the power level constant during the test period. Motion data was taken using a video and the deflection angle was post-processed using ProAnalyst motion analysis software. Figure 9 shows the curves recorded at the 10th, 15th, 20th and 25th repetition of a single prototype. We observed maximum of 0.3 s faster reaction in the first run of freshly annealed and tested actuator but the subsequent test runs of the same actuator showed no significant performance difference. We believe the speed difference in the first run is due to the initial reaction of the epoxy that holds the heater to the actuator surface. Figure 10 displays the repetition of the test with six different samples that are fabricated in the same conditions but different batches. At the transition temperature, the angular velocity varied from $62°$ to $65°$ s^{-1} regardless of the number of running cycles. The actuators displayed little variation in angular speed at the transition temperature. The temperature versus angle relationship shown in figure 11 clearly displays the transition temperature impact on the angular velocity: in between the beginning and the end of the austenite phase, which is, 55–$65\,°C$, the slope of the angular deflection is maximal.

4.2. Quasi-static tests

Even for basic calculations based on documented material properties, the thermo-mechanical model of the SMA requires extensive assumptions and over simplification of physical properties which risk misrepresenting the actuator properties. Here we measure the torque (blocked torque readings) induced by the shape memory effect in different models and control methods. Figure 12 shows the experimental setup for measuring the blocked torque at each angle. The actuator is attached to an x–z stage. The load applied by the actuator is read at 10 Hz by the precision balance and converted to a torque given. Figure 13 displays examples of the actuator in an unfolded $(0°)$ and fully folded $(180°)$ positions.

Figure 14 shows the power consumption by heating, and torque produced from the three actuator types. Most metals increase electrical resistivity with increases in temperature. For Ni–Cr wire, the change in resistivity from the room temperature $(20\,°C)$ to $93\,°C$, and to $204\,°C$, are 0. 8% and 2%, respectively. A larger temperature increase will induce a more significant resistance change. However, for the current testing, the maximum resistance change remains within 2% of the nominal resistance. The heater-carrying actuators consumes 3.6 W instead of 6.8 W at the maximum torque. Table 5 summarizes the experimental results of different actuator types.

5. Conclusion

This paper presents a fabrication process and experimental results of flat sheet torsional SMA actuators with high torque density, low profile, and improved response rates versus Joule heating. We introduce a new method for fabricating torsional actuators from 2D sheets using laser micromachining and annealing. These actuators exhibit high torque and energy densities without the need for auxiliary torque amplification mechanisms. Furthermore, by utilizing external heating
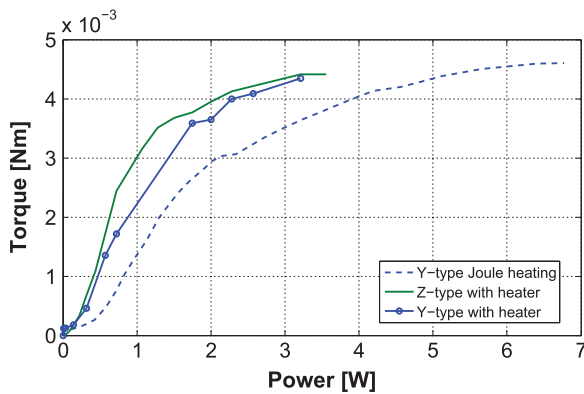
Figure 14. Torque versus power consumption for the three actuator prototypes.

Table 5. Performance comparison for both activation methods in Y-type actuators (average measurement of five samples).

	Ni–Cr coil heating	Joule heating
Maximum attainable blocked torque (N m)	0.0045	0.0047
Range of motion (deg)	0–180	0–180
Mass (kg)	35×10^{-6}	33×10^{-6}
Energy density (J kg^{-1})	241.1	210.8
Step response time constant (s)	2.5	3.1
Power consumption (W)	3.6	6.8

elements, we can achieve improved response rates and power efficiency—both of relevance to small-scale robots. The unique flat shape of this actuator allows it to be fully integrated in a thin robotic origami structure requiring large angular deflection. The newly suggested heating method introduced here is simple yet effective. Furthermore, its application on thin SMA sheet actuators allows concentrated and selective thermal activation. Future directions of current actuators include further advances on monolithic fabrication (i.e. depositing patterned Ni–Cr for concentrated heating), and machining and annealing adaptations for bidirectional actuators.

Acknowledgment

References

[1] Van Humbeeck J, Chandrasekaran M and Delaey L 1991 Shape memory alloys: materials in action *Endeavour* **15** 148–54
[2] Kohl M 2004 *Shape Memory Microactuators* (Berlin: Springer)
[3] Flomenblit J, Budigina N and Bromberg Y 1996 Two way shape memory alloy medical stent *US Patent Specification* 5,562,641
[4] Tung A, Park B, Koolwal A, Nelson B, Niemeyer G and Liang D 2006 Design and fabrication of tubular shape memory alloy actuators for active catheters *BioRob 2006: 1st IEEE/RAS-EMBS Int. Conf. on Biomedical Robotics and Biomechatronics 2006* pp 775–80
[5] Tung A, Park B, Liang D and Niemeyer G 2008 Laser-machined shape memory alloy sensors for position feedback in active catheters *Sensors Actuators* A **147** 83–92
[6] Morgan N 2004 Medical shape memory alloy applications—the market and its products *Mater. Sci. Eng.* A **378** 16–23
[7] Yoshida E, Murata S, Kokaji S, Tomita K and Kurokawa H 2000 Micro self-reconfigurable robotic system using shape memory alloy *DARS 2000: Proc. Int. Symp. on Distributed Autonomous Robotic Systems* pp 145–54
[8] Matsunaga T, Makishi W, Totsu K, Esashi M and Haga Y 2005 2-D and 3-D tactile pin display using SMA micro-coil actuator and magnetic latch *Transducers'05: 13th Int. Conf. on Solid-State Sensors, Actuators and Microsystems 2005. Dig. Tech. Papers* vol 1
[9] Mineta T, Mitsui T, Watanabe Y, Kobayashi S, Haga Y and Esashi M 2001 Batch fabricated flat meandering shape memory alloy actuator for active catheter *Sensors Actuators* A **88** 112–20
[10] Yoshikawa W, Sasabe A, Sugano K, Tsuchiya T, Tabata O and Ishida A 2006 Vertical drive micro actuator using SMA thin film for a smart button *MEMS 2006: IEEE Int. Conf. on Micro Electro Mechanical Systems 2006 (Istanbul)* pp 734–7
[11] Nakamura Y, Nakamura S, Ataka M, Fujita H and Miyazaki S 1996 Micromachining process for thin-film SMA actuators *EFTA'96: IEEE Conf. on Emerging Technologies and Factory Automation 1996* vol 2
[12] Cho M and Kim S 2005 Structural morphing using two-way shape memory effect of SMA *Int. J. Solids Struct.* **42** 1759–76
[13] Yang Y, Ye X and Guo S 2007 A New Type of Jellyfish-Like Microrobot *ICIT'07: IEEE Int. Conf. on Integration Technology 2007* pp 673–8
[14] Guo S and Ohira J 2003 A novel type of micropump using SMA actuator for microflow application *Nippon Robotto Gakkai Gakujutsu Koenkai Yokoshu (CD-ROM)* vol 21 p 1J2A
[15] Yoshida E, Murata S, Kokaji S, Kamimura A, Tomita K and Kurokawa H 2002 Get back in shape! a hardware prototype self-reconfigurable modular microrobot that uses shape memory alloy *IEEE Robot. Autom. Mag.* **9** 54–61
[16] Chiroiu V and Munteanu L 2006 A flexible beam actuated by a shape memory alloy ribbon *Proc. Rom. Acad.* A **4** 1–7
[17] Rogers C and Jia J 992 Formulation of a mechanical model for composites with embedded SMA actuators *Trans. ASME* **114** 670–6
[18] Leclercq S and Lexcellent C 1996 A general macroscopic description of the thermomechanical behavior of shape memory alloys *J. Mech. Phys. Solids* **44** 953–7
[19] Chaudhry Z and Rogers C 1991 Bending and shape control of beams using SMA actuators *J. Intell. Mater. Syst. Struct.* **2** 581
[20] Liang C and Rogers C 1992 A multi-dimensional constitutive model for shape memory alloys *J. Eng. Math.* **26** 429–43
[21] Liang C and Rogers C 1990 Design of shape memory alloy actuators *Intelligent Structures* vol 416 (Oxford: Elsevier Science)
[22] Liang C and Rogers C 1990 One-dimensional thermomechanical constitutive relations for shape memory materials *J. Intell. Mater. Syst. Struct.* **1** 207–34
[23] Boyd J and Lagoudas D 1996 A thermodynamical constitutive model for shape memory materials. Part I. The monolithic shape memory alloy and part II. The SMA composite material *Int. J. Plast.* **12** 805–73
[24] Menciassi A, Gorini S, Pernorio G and Dario P 2004 A SMA actuated artificial earthworm *ICRA'04: Proc. IEEE Int. Conf. on Robotics and Automation 2004* vol 4 pp 3282–7

[25] Kim B, Lee M, Lee Y, Kim Y and Lee G 2006 An earthworm-like micro robot using shape memory alloy actuator *Sensors Actuators* A **125** 429–37

[26] Koh J and Cho K 2010 Omegabot: biomimetic inchworm robot using SMA coil actuator and smart composite microstructures (SCM) *ROBIO: 2009 IEEE Int. Conf. on Robotics and Biomimetics* IEEE pp 1154–9

[27] Wang Z, Hang G, Li J, Wang Y and Xiao K 2008 A micro-robot fish with embedded SMA wire actuated flexible biomimetic fin *Sensors Actuators* A **144** 354–60

[28] Ikuta K 1990 Micro/miniature shape memory alloy actuator *Proc. 1990 IEEE Int. Conf. on Robotics and Automation, 1990* pp 2156–61

[29] Colli M, Bellini A, Concari C, Toscani A and Franceschini G 2006 Current-controlled shape memory alloy actuators for automotive tumble flap *IECON 2006—32nd Annual Conf. on IEEE Industrial Electronics* pp 3987–90

[30] Khidir E, Mohamed N, Nor M and Mustafa M 2007 A new concept of a linear smart actuator *Sensors Actuators* A **135** 244–9

[31] Elahinia M *et al* 2005 A temperature-based controller for a shape memory alloy actuator *J. Vib. Acoust.* **127** 285

[32] Sreekumar M, Nagarajan T and Singaperumal M 2008 Experimental investigations of the large deflection capabilities of a compliant parallel mechanism actuated by shape memory alloy wires *Smart Mater. Struct.* **17** 065025

[33] Sreekumar M and Singaperumal M 2009 A generalized analytical approach to the coupled effect of SMA actuation and elastica deflection *Smart Mater. Struct.* **18** 115026

[34] Yang S and Seelecke S 2008 Modeling and Analysis of SMA-Based Adaptive Structures *Proc. COMSOL Conf. (Boston)*

[35] Kuribayashi K 1989 Millimeter size joint actuator using shape memory alloy *IEEE Micro Electro Mechanical Systems, 1989, Proc., An Investigation of Micro Structures, Sensors, Actuators, Machines and Robots* pp 139–44

[36] Kohl M and Skrobanek K 1998 Linear microactuators based on the shape memory effect *Sensors Actuators* A **70** 104–11

[37] Kohl M, Dittmann D, Quandt E and Winzek B 2000 Thin film shape memory microvalves with adjustable operation temperature *Sensors Actuators* A **83** 214–9

[38] Kohl M, Skrobanek K, Goh C and Allen D 1996 Mechanical characterization of shape memory micromaterials *Proc. SPIE* **2880** 108

[39] Allen D, Leong T, Lim S and Kohl M 1997 Photofabrication of the third dimension of NiTi shape memory alloy microactuators *Proc. SPIE* **3225** 126

[40] Hawkes E, An B, Benbernou N, Tanaka H, Kim S, Demaine E, Rus D and Wood R 2010 Programmable matter by folding *Proc. Natl Acad. Sci.* **107** 12441

[41] Son H, Gu J, Park S, Lee Y and Nam T 2006 Design of new quadruped robot with SMA actuators for dynamic walking *SICE-ICASE, 2006 Int. Joint Conf.* pp 344–8

[42] MEMRY GmbH 2010 *Memry-metalle (Oct. 2010),* available at http://www.memry.com/

[43] Khajepour A, Dehestani H and Golnaraghi F 1987 A new shape memory allow rotary actuator: design and modelling *Linear Algebr.* B **14** 311

[44] Ali M and Takahata K 2010 Frequency-controlled wireless shape-memory-alloy microactuators integrated using an electroplating bonding process *Sensors Actuators* A **163** 363–72

[45] Abadie J, Chaillet N and Lexcellent C 2009 Modeling of a new SMA micro-actuator for active endoscopy applications *Mechatronics* **19** 437–42

[46] Kim S, Hawkes E, Choy K, Joldaz M, Foleyz J and Wood R 2009 Micro artificial muscle fiber using NiTi spring for soft robotics *IROS 2009: IEEE/RSJ Int. Conf. on Intelligent Robots and Systems, 2009* IEEE pp 2228–34

[47] Krulevitch P, Lee A, Ramsey P, Trevino J, Hamilton J and Northrup M 2002 Thin film shape memory alloy microactuators *J. Microelectromech. Syst.* **5** 270–82

[48] Aboudi J 1997 The response of shape memory alloy composites *Smart Mater. Struct.* **6** 1–9

[49] Oishi R, Yoshida H, Nagai H, Xu Y and Jang B 2002 Smart composite material system with sensor, actuator, and processor functions: a model of holding and releasing a ball *Proc. SPIE* **4701** 326